Electronic Absorption Spectroscopy of Aquated Transition Metal Ions

Introduction

The absorption of visible light by molecules and ions forms the basis for our perceptions of color. As with all molecular phenomena, the absorption of visible light is quantized and therefore only photons of certain energy (wavelength) are absorbed for a given chemical species. The absorption of visible light photons typically results in transitions between different ***electronic states***. As a result, spectroscopy involving visible light is often referred to as electronic absorption spectroscopy. In addition to visible light, photons in the near-UV and near-IR, although imperceptible to the human eye, can also result in electronic transitions leading to an energy range of ~45,000 cm^{-1} for electronic absorption (Figure 1).

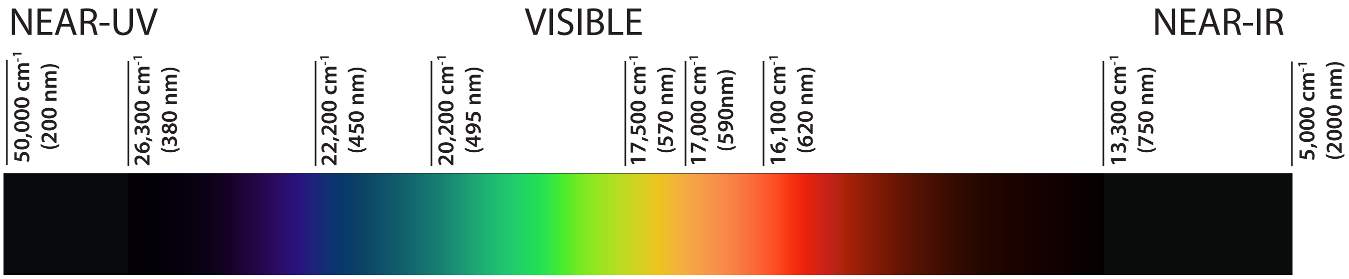
NEAR-UV
VISIBLE
NEAR-IR
50,000 cm-1 (200 nm)
26,300 cm-1 (380 nm)
22,200 cm-1 (450 nm)
20,200 cm-1 (495 nm)
17,500 cm-1 (570 nm)
17,000 cm-1 (590nm)
16,100 cm-1 (620 nm)
13,300 cm-1 (750 nm)
5,000 cm-1 (2000 nm)

Figure 1. Approximate range of the EM spectrum involved in electronic absorption.

Electronic transitions correspond to the promotion of a molecule or ion from a ground electronic state (ψ_e^g) to an excited electronic state (ψ_e^e) and can also be accompanied by vibrational transitions (sometimes termed ***vibronic transitions***). From an orbital standpoint, electronic transitions are most easily understood by considering the possible electron configurations resulting from excitation of a single electron from a filled molecular orbital to an unoccupied molecular orbital (Figure 2). Because organic molecules such as hydrocarbons contain sizable HOMO-LUMO gaps (> 28,000 cm^{-1}), electronic transitions in these molecules require relatively large amounts of energy pushing their absorptions into the near-UV. As a result, the compounds appear colorless to the naked eye.

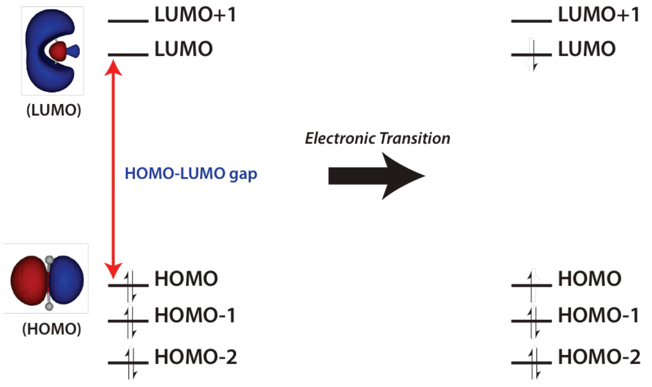
LUMO+1
LUMO
(LUMO)
HOMO-LUMO gap
Electronic Transition
HOMO
HOMO-1
HOMO-2
(HOMO)
LUMO+1
LUMO
HOMO
HOMO-1
HOMO-2

Figure 2. Simplified molecular orbital diagram for water showing the HOMO-LUMO transition.

One class of compounds that do show transitions in the visible region of the spectrum is transition metal complexes. In these species, the partial *d* orbital occupation gives rise to lower energy HOMO-LUMO gaps allowing transitions to occur with photons in the visible or near-IR. Such transitions account for the brilliant colors of many transition metal complexes (e.g. rubies). For simple transition metal ions, the number of absorption bands and their energies can be predicted using ***crystal field theory*** (***CFT***). The CFT model treats metal-ligand interactions as purely ionic resulting in interaction energies governed by simple electrostatics. Despite its simplicity, the CFT model is quite successful in describing a variety of transition metal complexes where a large degree of covalency is absent from the metal-ligand bonding. By using CFT and group theory, ***correlation diagrams*** can be developed which depict the energy of electronic states derived from different *d* electron configurations. It is transitions between these electronic states, termed ***ligand-field transitions***, that give rise to the observed visible/near-IR absorptions in transition metal complexes. One very useful example of a correlation diagram for transition metal complexes of octahedral *or* tetrahedral symmetry is the ***Tanabe-Sugano diagram*** (Figure 3). Tanabe-Sugano diagrams are drawn such that the energy of excited electronic states relative to the ground state (the *x*-axis) are plotted as a function of the crystal field strength (Δ or 10 *Dq*). Energy units in Tanabe-Sugano diagrams are expressed in terms of a factor that accounts for electron-electron repulsion in the free ion (one of the ***Racah parameters***, ***B***). These diagrams are of great value because they can be used to calculate Δ_o and B' for a given complex from experimental electronic absorption data.

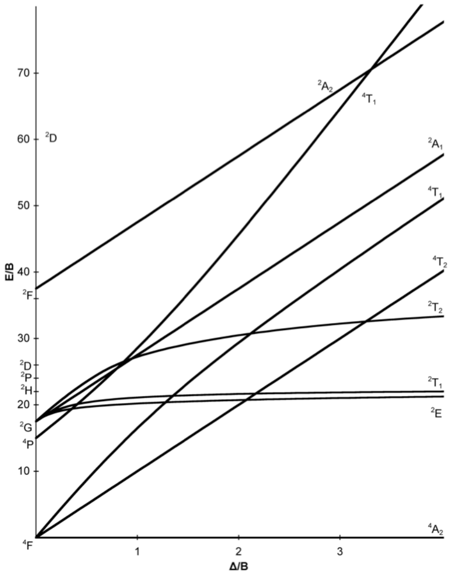

Figure 3. Tanabe-Sugano diagram for an octahedral d^3 metal ion such as Cr(III).

The intensity of an electronic absorption is determined by the ***oscillator strength, f***. The oscillator strength can be related to the energy of the absorption in wavenumbes ($\tilde{v}$) and the ***molecular extinction coefficient, ε***, as shown in Equation 1. The oscillator strength of the electronic transition is in turn related to the ***transition moment integral*** (Equation 2). Since electronic absorption typically occurs through an electric dipole mechanism, the ***electric dipole moment operator***, *μ*, appears in Equation 2.

$$f = 4.32 \times 10^{-9} \int \varepsilon \, d\tilde{v} \qquad (1)$$

$$M_e^{j \rightarrow k} = \int \psi_e^j \mu \psi_e^k \, d\tau \qquad (2)$$

Selection rules help us predict whether certain transitions will be allowed (i.e. have non-zero intensity). These rules result in part from the symmetry of the ground and excited state wavefunctions and that of the transition moment operator, *μ*. For transitions between electronic states comprising *d* orbital configurations there are two selection rules that need mention. The first, the ***spin multiplicity selection rule*** states that the spin multiplicity of the ground state and excited must be the same ($\Delta S = 0$). This rule can be understood by assuming that the spin component of the electronic wavefunction (ψ_s) is uncoupled to the orbital component (ψ_o). In this situation Equation 2 can be rewritten as shown in Equation 3, demonstrating that the spin selection rule is essentially an overlap integral. The spin selection rule can be relaxed through ***spin-orbit coupling*** (not discussed here), but electronic absorptions involving formally spin-forbidden transitions typically have very low intensities.

$$M_e^{j\rightarrow k} = \int \psi_s^j \psi_s^k \, d\tau \cdot \int \psi_o^j \mu \psi_o^k \, d\tau \qquad (3)$$

The second selection rule of importance to transition metal complexes is the ***LaPorte Selection rule***. This rule states that only transitions from states with wavefunctions of even (*gerade*) symmetry to states with wavefunctions of odd (*ungerade*) symmetry, or vice versa, are allowed. This rule follows straightforwardly from Equation 2. The consequence of the LaPorte selection rule is that ligand field transitions (*d* to *d*) in octahedral complexes are forbidden because all *d* orbitals have *gerade* symmetry. This rule can be relaxed through a variety of mechanisms including *d-p* mixing (tetrahedral complexes) and vibronic coupling. In practice, LaPorte-forbidden transitions have weak intensities ($\varepsilon \approx 1$ - 500), but are still much stronger than spin-forbidden transitions ($\varepsilon < 0.1$).

Detection of electronic absorption is most conveniently accomplished through use of a spectrophotometer. The spectrophotometer produces and directs radiation of a given wavelength through the sample of interest and measures the resulting ***absorbance, A***. As a result of electronic absorption of molecules in an optically transparent medium (such as solvent), the intensity of incident radiation, I_0, passing through the sample is decreased to some value, I. The absorbance is defined as the $\log_{10}$ of (I_0/I), which is described by ***Beer's Law*** as shown in Equation 4.

$$\log \frac{I_0}{I} = A = \varepsilon c l \qquad (4)$$

In this experiment the electronic absorption spectrum of several aquated transition metal ions $[M(H_2O)_6]^{n+}$ will be recorded and analyzed. By determining the extinction coefficients for each complex using a Beer's Law plot and comparing it with literature values, the number of waters of hydration for each of the starting sulfate salts, $MSO_4 \cdot xH_2O$, will be calculated. In addition, the absorption data obtained for each complex will be used to calculate the crystal-field splitting parameter, Δ_o, by analysis of the appropriate Tanabe-Sugano diagram.

Procedure

The teaching assistant will assign a certain sulfate salt (Cr^{III}, Fe^{II}, Co^{II}, Ni^{II}, or Cu^{II}) to each student. Be sure to note the correct ionic formula for each. Students will then prepare solutions of known concentrations for the assigned sulfate salt using volumetric technique (the molecular weight used should neglect waters of hydration). At least 5 solutions of known concentration should be prepared in order to generate a Beer's Law plot with substantial data points to accurately determine the molar absorptivity. The approximate masses required to generate stock solutions of appropriate concentration for each sulfate salt appear in Table 1 below. These amounts should be dissolved in deionized water to a volume of 50 mL. Serial dilutions comprising 80%, 60%, 40%, and 20% of the concentration of the stock solution should then be made to create a total of 5 solutions to be measured.

Table 1. Amounts of each metal sulfate used to generate the initial stock solution.

Metal Ion	Mass (g)
Cr^{III}	0.5
Fe^{II}	5.3
Co^{II}	1.5
Ni^{II}	1.5
Cu^{II}	1.0

Once dissolved in solution (be patient!), the sulfate salts will form the corresponding hexaaqua ions, $[M(H_2O)_6]^{n+}$. Record the electronic absorption spectrum (scan range should be 1500 – 300 nm) of the assigned metal ion at each of the five concentrations and determine the molar absorptivity for each major peak in the spectrum with a λ_{max} above 300 nm. Once this is complete, save the spectra. Each student will need a copy of all five different metal ion spectra. The TA can facilitate sharing of the electronic files. Once all work is complete, dispose of the metal ion solutions in the appropriate receptacle.

In addition to the aqua complexes, the TA will prepare and record the spectra of two tetrahedral metal complexes in acetonitrile, $[NiCl_4]^{2-}$ and $[CuCl_4]^{2-}$ (each as their tetrabutylammonium salt). Each student should also obtain a copy of these spectra.

Questions

1. Based on the data obtained by each lab group, determine as well as possible the complete formula (including waters of hydration) for each metal sulfate by comparing the molar absorptivities with those of the literature values found in the appendix. [Note that the measured ε values must necessarily be less than those in the literature because the molecular weights used in this experiment fail to account for the waters of hydration.]

2. Check the numbers of waters resulting from your calculation with those on the commercial bottle (supplied after the lab by the TA). How closely do they agree? Comment on possible systematic error introduced during the experiment.

3. Draw the *d*-orbital splitting diagrams for each $[M(H_2O)_6]^{n+}$ complex.

4. Do the number of transitions predicted by the Tanabe-Sugano diagrams (Appendix) match those obtained for each metal ion? Comment on possible discrepancies.

5. Using the Tanabe-Sugano diagrams in the appendix, determine Δ_o and B' for $[Ni(H_2O)_6]^{2+}$ and $[Cr(H_2O)_6]^{3+}$. What is Δ_o for $[Cu(H_2O)_6]^{2+}$ and $[Fe(H_2O)_6]^{2+}$? Are Tanabe-Sugano diagrams necessary to determine the crystal field splitting parameters for these complexes?

6. Draw the *d*-orbital splitting diagrams for each $[MCl_4]^{2-}$ complex.

7. Comment on the differences in energy and intensity between the absorption bands of the aqua complexes and those of the tetrachlorometallate anions.

8. Calculate Δ_o and B' for $[NiCl_4]^{2-}$ using the appropriate Tanabe-Sugano diagram found in the Appendix or at:

   http://wwwchem.uwimona.edu.jm:1104/courses/Tanabe-Sugano/TSspread.html

   In order to do so, you must use the following relationship:

$$\text{octahedral } d^n \Leftrightarrow \text{tetrahedral } d^{10-n}$$

Appendix

Literature values[1] for $[M(H_2O)_6]^{n+}$ in water:

Metal Complex	**ε ($M^{-1}cm^{-1}$)**
$[Cr(H_2O)_6]^{3+}$	15.8, 17.5
$[Fe(H_2O)_6]^{2+}$	1.3
$[Co(H_2O)_6]^{2+}$	1.3, 4.9
$[Ni(H_2O)_6]^{2+}$	2.0, 2.2, 5.0
$[Cu(H_2O)_6]^{2+}$	11.3

Tanabe-Sugano diagrams for selected *d* electron configurations in octahedral geometry:

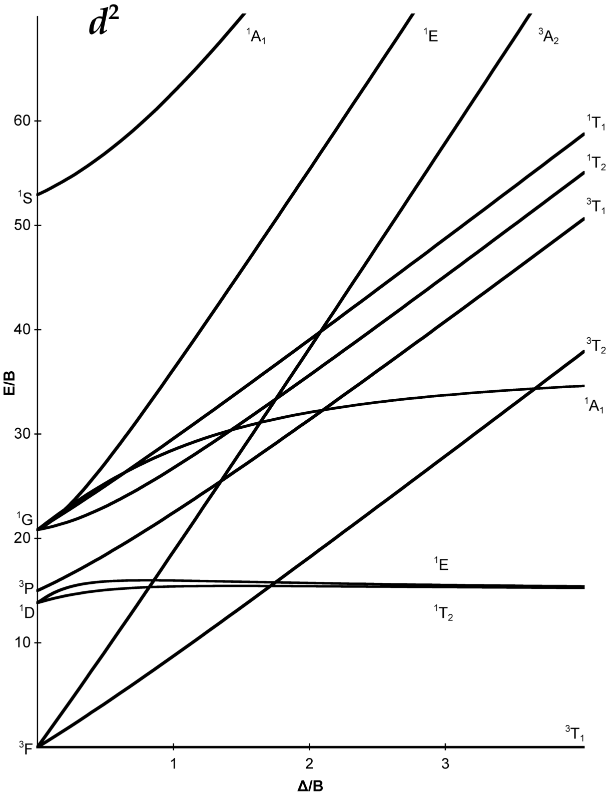

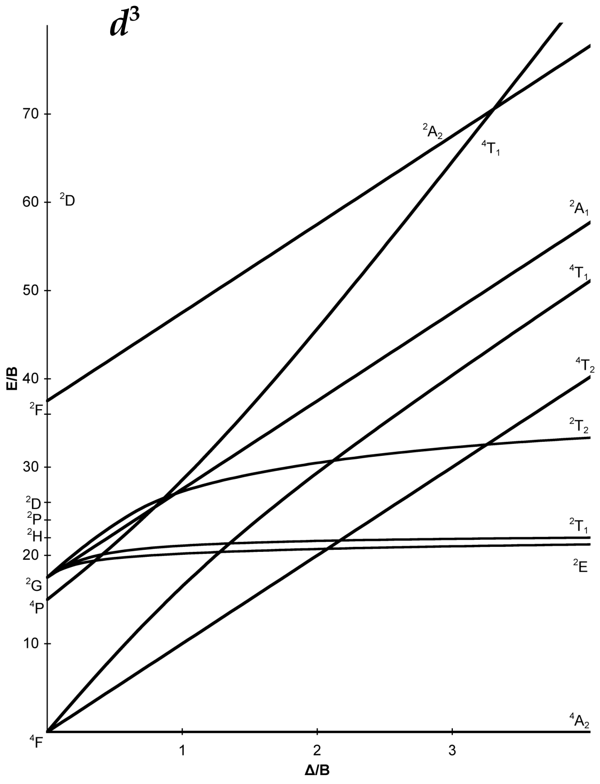

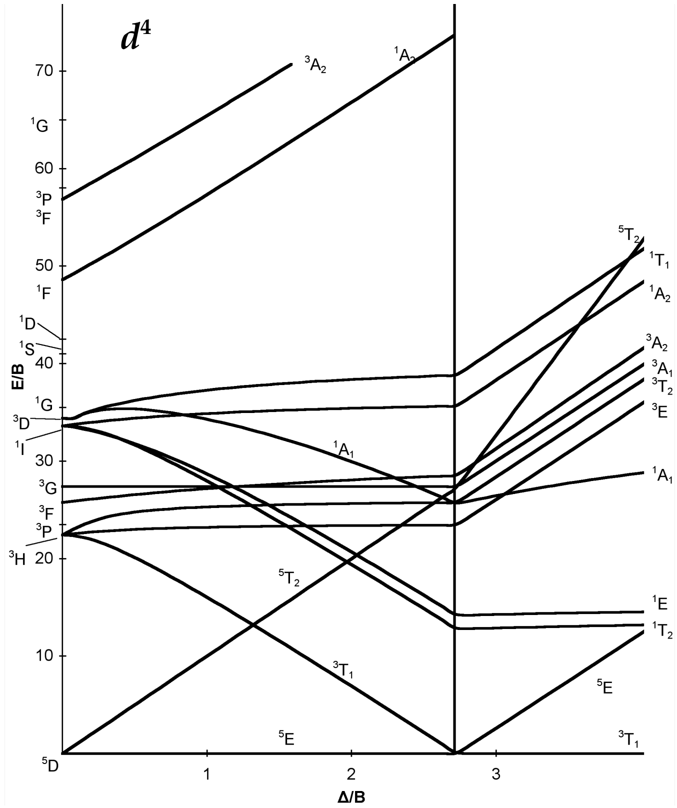
d^4
E/B
70
^1G
60
^3P
^3F
50
^1F
^1D
^1S
40
^1G
^3D
^1I
30
^3G
^3F
^3P
^3H
20
10
^5D
$^3A_2$
$^1A_2$
$^5T_2$
$^1T_1$
$^1A_2$
$^3A_2$
$^3A_1$
$^3T_2$
^3E
$^1A_1$
$^1A_1$
$^5T_2$
^1E
$^1T_2$
$^3T_1$
^5E
^5E
$^3T_1$
1
2
3
Δ/B

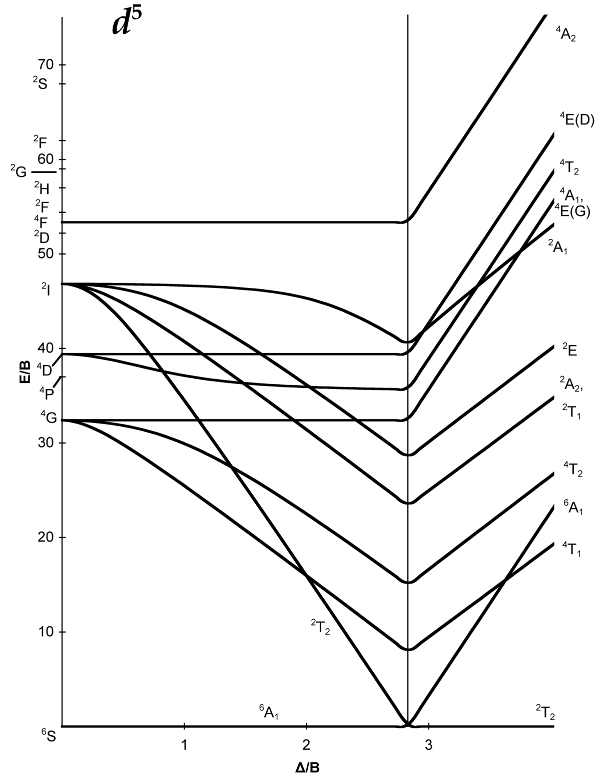
d^5
E/B
70
^2S
^2F
60
^2G
^2H
^2F
^4F
^2D
50
^2I
40
^4D
^4P
^4G
30
20
10
^6S
$^4A_2$
$^4E(D)$
$^4T_2$
$^4A_1$,
$^4E(G)$
$^2A_1$
^2E
$^2A_2$,
$^2T_1$
$^4T_2$
$^6A_1$
$^4T_1$
$^2T_2$
$^6A_1$
$^2T_2$
1
2
3
Δ/B

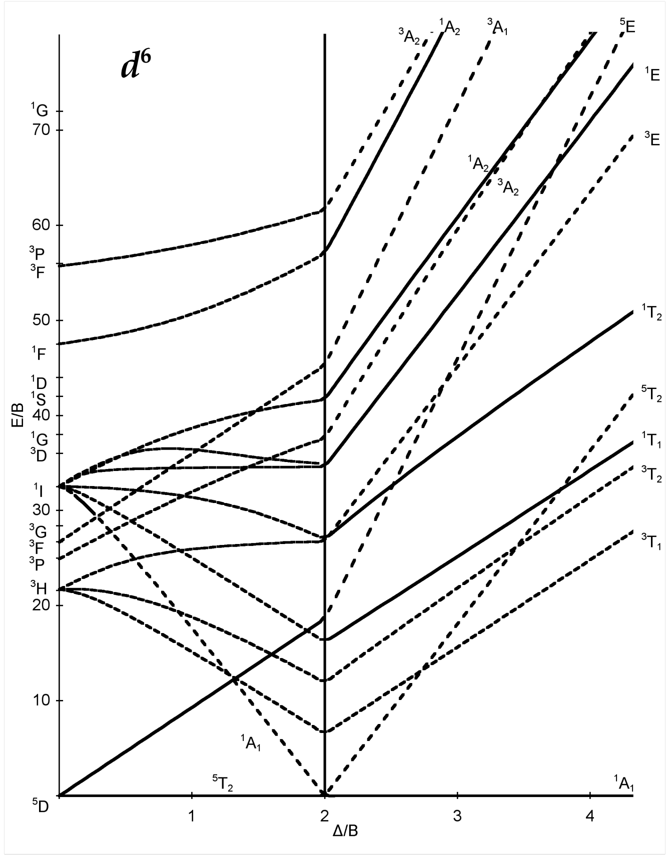
d^6
E/B
^1G
70
60
^3P
^3F
50
^1F
^1D
^1S
40
^1G
^3D
^1I
30
^3G
^3F
^3P
^3H
20
10
^5D
$^3A_2$
$^1A_2$
$^3A_1$
^5E
^1E
^3E
$^1A_2$
$^3A_2$
$^1T_2$
$^5T_2$
$^1T_1$
$^3T_2$
$^3T_1$
$^1A_1$
$^5T_2$
$^1A_1$
1
2
3
4
Δ/B

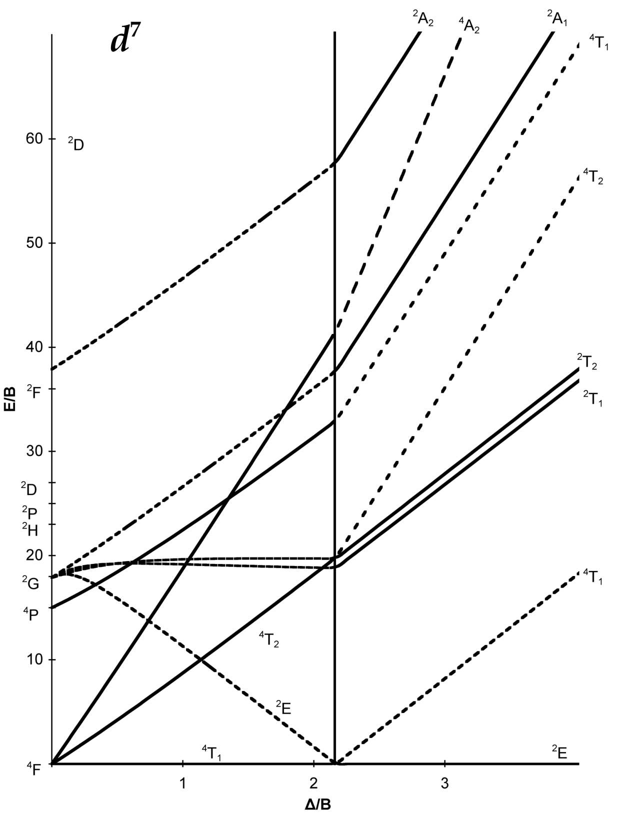
d^7
E/B
60
^2D
50
40
^2F
30
^2D
^2P
^2H
20
^2G
^4P
10
^4F
$^2A_2$
$^4A_2$
$^2A_1$
$^4T_1$
$^4T_2$
$^2T_2$
$^2T_1$
$^4T_1$
$^4T_2$
^2E
$^4T_1$
^2E
1
2
3
Δ/B

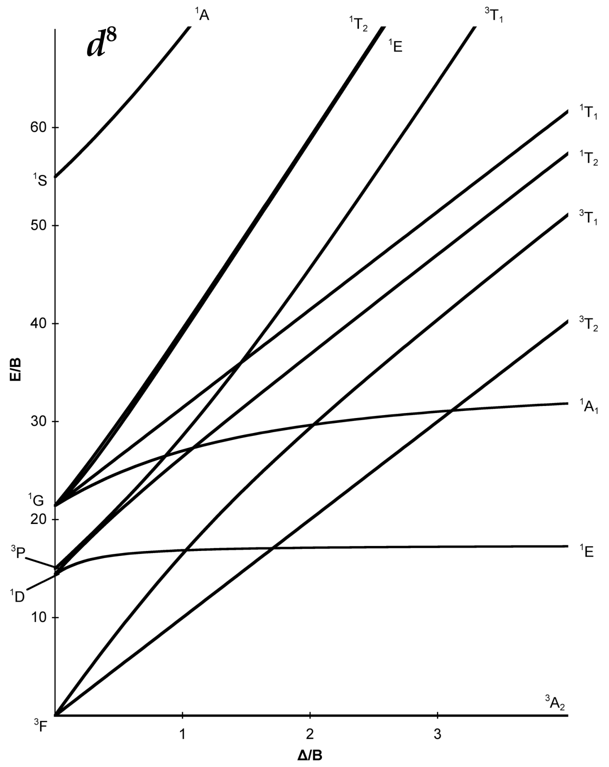

References

(1) Figgis, B. N. *Introduction to Ligand Fields*, Wiley-Interscience, New York, 1966.